Eur. Phys. J. C (2023) 83:860
https://doi.org/10.1140/epjc/s10052-023-12030-8

THE EUROPEAN PHYSICAL JOURNAL C

Regular Article - Theoretical Physics

Theoretical and observational prescription of warm-inflation in FLRW universe with torsion

Madhukrishna Chakraborty[a], **Gopal Sardar**[b], **Akash Bose**[c], **Subenoy Chakraborty**[d]

Department of Mathematics, Jadavpur University, Kolkata 700032, India

Received: 26 June 2023 / Accepted: 12 September 2023

Abstract The paper deals with Warm Inflationary scenario in FLRW with torsion both from theoretical and observational point of view. In the background of flat FLRW model the Hubble parameter is found to be proportional to the torsion function and warm inflation is examined both in weak and strong dissipation regimes for the power law choice of potential using slow-roll approximation with quasi-stable criteria for radiation. The slow-roll parameters, no.of e-folds, scalar spectral index, and tensor-to-scalar ratio are determined in the present model for mainly three choices of the dissipation coefficient Γ using the Planck data set. Finally, we focus on single-field chaotic quartic potential with the above choices of the dissipation coefficient to confront the warm inflation observational predictions directly with the latest observational data set.

1 Introduction

Series of cosmological observations namely Cosmic Microwave Background [1,2], Large Scale Structures [3,4], Baryon Acoustic Oscillation [5,6], both strong and weak lensing [7,8], galaxy cluster number counts [9], gravitational waves detections [10,11] etc, suggest that the universe expanded from an early dense and hot state. Subsequently, in 1981, Alan Guth put forward his theory of an exponentially expanding universe while in a supercooled vacuum state, which later came to be known as the *Inflation* [12]. Inflationary paradigm is one of the most well-accepted descriptions of the early universe just after Big Bang. The hypothesis of cosmic inflation in the early universe successfully solves the problems associated with standard big bang model like Horizon and Flatness problem [13]. Besides solving these problems cosmic inflation also explains the origin of CMB anisotropies and the large scale structure of the universe [14,15].

In a standard picture of inflation known as Cold Inflation, a scalar field ϕ (*inflaton*) slowly rolls down along a flat potential, giving rise to the desired amount of inflation.The inflaton field interacts with other field degrees of freedom much weakly and becomes unable to prevent the dilution of any pre-existing or newly formed radiation and as a result, there is a period of supercooling. Another type of inflation, known as *Warm Inflation* (WI) [16,17] attracted the interest of the cosmologists in which there is no separate reheating phase, and the interaction between the inflaton and other fields is more prominent to produce quasi-stationary thermalized radiation bath during inflation. Hence the thermal fluctuations in the radiation bath is the prime source of density fluctuations and it is transported to the inflaton field as adiabatic curvature perturbations. Further in WI, it is feasible to have a strong coupling between the inflaton field and other fields to have an appreciable amount of radiation production, preserving the required flatness of the potential. As a result, the supercooling of the universe as observed in cold inflation is compensated by the radiation production and the universe makes a smooth transition from the accelerated era of expansion (inflationary epoch) to radiation dominated era in WI without having any preheating era.

The standard cosmology in FLRW model has been a debating issue due to a series of observational evidences for the last two decades. Attempts to resolve this issue or to explain the present accelerated expansion have been continuing in two directions – introduction of exotic matter (known as dark energy) in the framework of Einstein gravity or modification of Einstein gravity theory itself. The second approach modifies the geometric part of the Einstein field equations and is termed as modified gravity theory. The present torsion theory

[a] e-mail: chakmadhu1997@gmail.com
[b] e-mail: gopalsardar.87@gmail.com
[c] e-mail: bose.akash13@gmail.com
[d] e-mail: schakraborty.math@gmail.com (corresponding author)

Published online: 26 September 2023

is an example of it. Cartan in 1922 developed this extension of Einstein's theory of gravity also known as Einstein- Cartan theory (ECT) by interpreting intrinsic angular momentum or spin of the matter in terms of torsion. Later in 1960 s ECT emerged as the simplest classical modification of Einstein's theory [18]. In contrast to general relativity, space-time in ECT contains asymmetric affine connection having symmetric Christoffel symbols in Riemannian geometry. In particular, the antisymmetric part of the affine or non-Riemannian connection characterizes the torsion. Hence, the gravitational pull is not only described by the metric tensor but also by the independent torsion field. From the geometric point of view, curvature tends to bend the space-time while torsion twists it. On the other hand from physical point of view presence of matter cause the curvature of the space-time while intrinsic angular momentum of matter characterizes the torsion. However introduction of torsion field does not allow the space-time to be homogeneous and isotropic which is the common choice for standard cosmology, rather it introduces anisotropic degrees of freedom. To overcome this unfavorable situation a typical vectorial form of the torsion field has been introduced in the recent past. In this case, the space-time torsion fields and the associated matter spin are completely determined by a homogeneous scalar function. This modified torsion field preserves the symmetry of the associated Ricci curvature tensor (in FLRW model) and hence the symmetry of Einstein tensor and energy–momentum tensor. Subsequently, after the discovery of quantum spin, Kibble and Sciama [19] reintroduced this notion in general relativity and is now known as ECKS theory. The ECKS theory of gravity is a natural extension of GR by including the spin and has a natural physical interpretation in the context of the Poincare group [20]. Due to torsion of space-time there was a gravitational repulsive force in the early universe, and as a consequence torsion prevents the initial cosmological singularity i.e, the universe expands from a finite minimum size [21,22]. In cosmology, due to high symmetry of the FLRW model, the torsion can be described by a scalar field (known as torsion field). Recently it has been shown how torsion can influence the standard evolution in cosmology, particularly low-redshift constraints by weak torsion field, effect of torsion field on late-time cosmology. Though it is hard to have an experimental evidence of the torsion field, particularly at high energy density yet there are predictive studies of the torsion field in inflationary scenario and in gravitational waves. Recently, it has been examined whether torsion field favors early inflationary epoch by analyzing scalar and tensor perturbation theory and by estimating the spectral index [23]. A non-Riemannian geometrical extension of GR is torsion which allows spin degrees of freedom of the matter and the twisting of space-time. Cosmological models with torsion are important both at early eras (i.e, high redshift z) and at the present phase of evolution. In the present work, we have carried the theoretical and observational study of warm inflation in FLRW with torsion to study the nature of slow-roll parameters, compare our results with results in literature and to explore the effect of torsion on the inflaton field and hence on the slow-roll approximations to determine tensor-to-scalar ratio. There lies the motivation behind connecting or studying warm inflation in the presence of torsion.

The layout of the work is: Sect. 2 gives a short account of FLRW model with torsion. Section 3 deals with the basics of Warm Inflation. Study of warm inflation in presence of torsion has been dealt with in Sect. 4 both from theoretical and observational point of view. The paper ends with summary and concluding remarks in Sect. 5.

2 A brief overview of FLRW with torsion

In theoretical physics, the Einstein–Cartan theory, also known as the Einstein–Cartan–Sciama–Kibble theory is an extension of general theory of relativity in the sense that it takes into account the role of torsion in spacetime. It was first developed by Cartan in 1922 with a view to propose torsion as the macroscopic manifestation of the intrinsic angular momentum of matter and is mainly based on the asymmetric affine connection for the space-time, different from the symmetric Christoffel symbols of Riemannian spaces [24,25].

Torsion tensor is identified by the antisymmetric component of the affine connection given by

$$S^a_{bc} = \Gamma^a_{[bc]} \tag{1}$$

where $S^a_{bc} = S_{[bc]}$ is the torsion tensor, and it vanishes without torsion. Employing the condition, $\nabla_c g_{ab} = 0$ i.e the metric tensor is covariantly constant, the generalized connection can be decomposed into a symmetric and an antisymmetric part as

$$\Gamma^a_{bc} = \tilde{\Gamma}^a_{bc} + K^a_{bc} \tag{2}$$

where $\tilde{\Gamma}^a_{bc}$ defines the Christoffel symbols and K^a_{bc} is the contortion tensor given by

$$\begin{aligned} K_{abc} &= S_{abc} + S_{bca} + S_{cba} = S_{abc} + 2S_{(bc)a} \\ &\text{with } K_{abc} = K_{[ab]c} \end{aligned} \tag{3}$$

Hence torsion can be considered as a connection between intrinsic angular momentum of matter and geometry of spacetime. The antisymmetry of the torsion tensor leads to one non-trivial contraction giving rise to torsion vector

$$S_a = S^b_{ab} (= -S^a_{ba}) \tag{4}$$

and consequently, for the contortion tensor we have

$$K^{b}_{ab} = 2S_a = -K^{\ b}_{ab} \tag{5}$$

Here we consider homogeneous and isotropic FLRW spacetime with line element

$$ds^2 = -dt^2 + a^2(t)\left[\frac{dr^2}{1-Kr^2} + r^2\left(d\Theta^2 + sin^2\Theta d\Phi^2\right)\right] \tag{6}$$

where $a(t)$ is the scale factor, K is the curvature index, $H = \frac{\dot{a}}{a}$ is the Hubble parameter and 'overdot' denotes differentiation with respect to cosmic time 't'. In case of spatially homogeneous and isotropic FLRW spacetime torsion vector fully characterizes the torsion tensor and hence the contortion tensor also. For this spacetime the torsion vector can be expressed as [26–29]

$$S_a = -3\Psi u_a, \tag{7}$$

where $\Psi(t)$ is a scalar function and u_a is the four-velocity field along the tangent to a congruence of timelike curves. The torsion tensor and the Contortion tensor can be written as

$$S_{abc} = 2\Psi h_{a[b}u_{c]}, \tag{8}$$

$$K_{abc} = 4\Psi u_{[a}h_{b]c}. \tag{9}$$

where h_{ab} is the metric of the three-space. The torsion vector is timelike, and the sign of Ψ, the scalar function indicates the relative orientation between the torsion and 4-velocity u_a. Precisely if $\Psi < 0$, torsion vector is future directed, while if $\Psi > 0$ it is past directed [30]. Moreover, the matter conservation equation in FLRW model assumes the form [22]

$$T^{b}_{a;b} = -4\Psi T_{ab}u^b \tag{10}$$

which can explicitly be written for perfect fluid as

$$\dot{\rho} + 3(H + 2\Psi)(p + \rho) = 4\Psi\rho \tag{11}$$

where ρ is the energy density and p is the thermodynamic pressure of the perfect fluid. Hence, the modified Friedmann equations due to torsion for flat FLRW spacetime can be written as

$$3H^2 = \kappa\rho - 12\Psi^2 - 12H\Psi \tag{12}$$

$$2\dot{H} = -\kappa(p + \rho) - 4\dot{\Psi} + 8\Psi^2 + 4H\Psi \tag{13}$$

The Einstein's field equations with interacting two fluids can be written as:

$$3H^2 = \rho + \rho_f \tag{14}$$

$$2\dot{H} + 3H^2 = -p - p_f \tag{15}$$

with the conservation equations given by:

$$\dot{\rho} + 3H(p + \rho) = Q \tag{16}$$

$$\dot{\rho_f} + 3H(\rho_f + p_f) = -Q \tag{17}$$

where $Q = \frac{\Gamma}{3H}$ (Γ is the dissipation coefficient, H is the Hubble parameter) and

$$\rho_f = -12\Psi^2 - 12H\Psi \tag{18}$$

$$p_f = 4\Psi^2 + 8H\Psi + 4\dot{\Psi} \tag{19}$$

3 Warm inflationary scenario: the basic equations involved

In this work, WI is considered in the background of spatially flat FLRW spacetime geometry having matter component as inflaton (a scalar field with self-interacting potential) which interacts with radiation [16]. The Friedmann equations governing this warm inflation can be written as

$$3H^2 = (\rho_\phi + \rho_r), \quad 2\dot{H} = -(\rho_\phi + p_\phi) - (\rho_r + p_r) \tag{20}$$

(here we choose $c = 1, \kappa = 8\Pi G = 1$). $\rho_\phi = \frac{1}{2}\dot{\phi}^2 + V(\phi)$ is the energy density of the homogeneous scalar field $\phi = \phi(t)$, $V(\phi)$ is the self interacting potential, ρ_r is the energy density of the radiation fluid. p_ϕ and p_r are the pressure of the scalar field and radiation fluid respectively and $p_r = \frac{1}{3}\rho_r$, $p_\phi = \frac{1}{2}\dot{\phi}^2 - V(\phi)$.

The total energy density $\rho = \rho_\phi + \rho_r$ satisfies the relation $\dot{\rho} + 3H(p + \rho) = 0$. In warm inflation, due to the decay of the scalar field, which is essentially a dissipative process, energy is transferred from the field to radiation, and this process is governed by the following energy conservation equations:

$$\dot{\rho}_\phi + 3H(p_\phi + \rho_\phi) = -\Gamma\dot{\phi}^2 \tag{21}$$

$$\dot{\rho}_r + 3H(p_r + \rho_r) = \Gamma\dot{\phi}^2 \tag{22}$$

Using the above explicit expressions of energy density and pressure of the scalar field, Eq. (21) can be reformulated as the generalised Klein–Gordan equation for the scalar field as

$$\ddot{\phi} + 3H(1 + Q)\dot{\phi} + V'(\phi) = 0 \tag{23}$$

where $Q = \frac{\Gamma}{3H}$ denotes the ratio of the radiation production to the expansion rate. The quantity Q represents the effectiveness at which the inflation energy is transformed to radiation energy. Assuming the cosmological expansion to be quasi-de Sitter, scalar field energy is predominant over the radiation

energy density i.e $\rho_\phi \gg \rho_r$, and the kinetic term of the scalar field is much smaller as compared to the potential term.

Further assuming the production of the radiation component to be quasi-stable during the inflationary era i.e employing the conditions $\dot{\rho}_r \ll H\rho_r$ and $\dot{\rho}_r \ll \Gamma\dot{\phi}^2$, Eqs. (20)–(23) can be approximated as

$$3H^2 \simeq V(\phi) \tag{24}$$

$$\dot{\phi} \simeq -\frac{V'(\phi)}{3H(1+Q)} \tag{25}$$

$$\rho_r \simeq \frac{\Gamma\dot{\phi}^2}{4H} = C_\gamma T^4 \tag{26}$$

where T is the temperature of the radiation bath, $C_\gamma = \frac{\pi^2 g_*}{30}$ is the Stefan–Boltzmann constant, g_* is the number of degrees of freedom of the radiation fluid, 'prime' denotes differentiation with respect to scalar field ϕ. Typically, during the scenario of warm inflation we can identify two regimes; called the weak dissipative regime (WDR) where $Q \ll 1$ (or $\Gamma \ll 3H$) and the strong dissipative regime (SDR) where $Q \gg 1$ (or $\Gamma \gg 3H$). In the present work, we consider Γ to be a function of the scalar field i.e, $\Gamma = \Gamma(\phi)$, explicitly $\Gamma = \Gamma_0\phi^m$. Moreover calculations are carried out considering two other choices of Γ namely $\Gamma = \Gamma_0 T^m$ i.e, Γ as a function of the temperature of thermal bath [31] and $\Gamma = \Gamma_0\frac{T^m}{\phi^{m-1}}$ i.e, Γ as a function of both ϕ and T where Γ_0 is connected to the dissipative microscopic dynamics. For $m = -1$, $\Gamma = \Gamma_0\frac{\phi^2}{T}$, the form corresponds to the dissipative coefficient in the non-SUSY case, for $m = 0$, $\Gamma = \Gamma_0\phi$ which corresponds to the SUSY case with an exponentially decaying propagator, for $m = 1$, $\Gamma = \Gamma_0 T$ which corresponds to the high temperature SUSY case [32]. Further, the motivation behind choosing Γ in power law dependence on temperature comes from [33] where the authors have used recent results of sphaleron rate in classical lattice gauge theory which predicts a power law (particularly cubic) dependence of Γ on T. One may also refer [34] where a simple functional form of Γ is given that is dependent on the temperature T of the thermal bath and the amplitude ϕ of the inflaton field. There lies the motivation behind choosing the dissipative models in this manner.

With the help of the above equations, the first slow-roll parameter can be expressed as

$$\epsilon_1 = \frac{1}{2(1+Q)}\left(\frac{V'^2}{V^2}\right) = -\frac{\dot{H}}{H^2} \tag{27}$$

and the other two slow-roll parameters can be expressed as

$$\eta = \frac{1}{(1+Q)}\frac{V''}{V}, \quad \beta = \frac{1}{(1+Q)}\frac{V'\Gamma'}{V\Gamma} \tag{28}$$

N, the number of e-folds given by

$$N = \int_{t_\star}^{t_e} H\mathrm{d}t = \int_{\phi_\star}^{\phi_e}\frac{H}{\dot{\phi}}\mathrm{d}\phi = -\int_{\phi_\star}^{\phi_e}\frac{(1+Q)V}{V'}\mathrm{d}\phi \tag{29}$$

is the measure of the amount of cosmic expansion during the inflationary epoch. The subscripts 'e' and '$\star$' denote the quantity at the end of the inflation and at the horizon crossing time respectively. On the other hand, the source of density fluctuations correspond to thermal fluctuations due to the presence of radiation fluid in warm inflation dynamics. Thermal fluctuations depend on the fluid temperature T while quantum fluctuations are dependent on the Hubble parameter H. In warm inflationary scenario, since the fluid temperature T is greater than the Hubble parameter H it hints that the thermal fluctuations dominate over the quantum fluctuations. This explains the Large Scale Structure of the universe. The scalar spectral index n_s defined by $n_s = 1 + \frac{\mathrm{d}\ln P_s}{\mathrm{d}\ln k}$ [32] can be expressed in terms of the slow-roll parameters as

$$n_s = 1 - \frac{9Q+17}{4(1+Q)}\epsilon_1 - \frac{9Q+1}{4(1+Q)}\beta + \frac{3}{2}\eta \tag{30}$$

As per the latest observational data or the precise values as favored by the Planck data set [35], the amplitude of the scalar perturbation at the horizon crossing is given by $P_s = 2.17 \times 10^{-9}$ [36,37] and value of the spectral index n_s is 0.9649 ± 0.0042 TT,TE,EE+lowE+lensing at 68% CL. Amplitude of tensor perturbation is given by $P_t = 8H^2$. The tensor-to-scalar ratio is $r = \frac{P_t}{P_s} = \frac{16\epsilon_1 H}{(1+Q)^{\frac{3}{2}}T}$ and in 95% CL the upper limit of the tensor-to-scalar ratio is 0.10.

4 Warm inflation in FLRW universe with torsion

In the literature, the usual fluid is considered as the radiation fluid and the effective fluid is taken as the inflaton fluid. However in the present context one may show that this assumption is inconsistent with the quasi-stable production of the radiation component. The detailed calculation in this regard has been shown in Appendix. Henceforth we consider the usual fluid as inflaton and the effective fluid as radiation. Mathematically it can be written as,

$$\rho = \rho_\phi = \frac{1}{2}\dot{\phi}^2 + V(\phi), \tag{31}$$

$$p = p_\phi = \frac{1}{2}\dot{\phi}^2 - V(\phi), \tag{32}$$

$$\rho_f = \rho_r = -12\Psi^2 - 12H\Psi, \tag{33}$$

$$p_f = p_r = 4\Psi^2 + 8H\Psi + 4\dot{\Psi}. \tag{34}$$

(Equations (33) and (34) follow from Eqs. (18 and 19)). So the evolution equations of two-fluid can be separately written as

$$\dot{\rho_\phi} + 3(H + 2\Psi)(\rho_\phi + p_\phi) = 4\Psi\rho_\phi \tag{35}$$

$$\text{i.e.,}\quad \dot{\rho_\phi} + 3H(\rho_\phi + p_\phi) = -2\Psi(\rho_\phi + 3p_\phi) = -\Gamma\dot{\phi}^2 \tag{36}$$

$$\text{and } \dot{\rho}_r + 4H\rho_r = \Gamma\dot{\phi}^2 = 2\Psi(\rho_\phi + 3p_\phi) \tag{37}$$

Now, using the slow-roll approximations the interaction term $\Gamma\dot{\phi}^2$ can be approximated as $\Gamma\dot{\phi}^2 = 2\Psi(\rho_\phi + 3p_\phi) = 4\Psi(\dot{\phi}^2 - V(\phi)) \simeq -4\Psi V(\phi)$. It should be noted that $\Gamma\dot{\phi}^2$ is positive for future directed torsion function and consequently energy is transferred from the scalar field to radiation fluid. So the evolution equation (37) of the radiation fluid can be rewritten as

$$\dot{\rho}_r + 4H\rho_r \simeq -4\Psi V(\phi) \tag{38}$$

Now assuming the quasi-stable conditions ($\dot{\rho}_r << H\rho_r$), one can approximate the above equation as

$$H\rho_r \simeq -\Psi V(\phi). \tag{39}$$

Finally using Eqs. (24) and (33) in Eq. (39), the Hubble parameter in terms of the torsion function (Ψ) can be written as

$$H \simeq \frac{-4}{3}\Psi. \tag{40}$$

In this work, a generalized power law potential in form of $V = V_0\phi^n$ is chosen to study the nature of weak and strong dissipative regime in torsion gravity. Thus the inflaton field ϕ is related to the torsion function Ψ by the relation

$$\phi = \left(\frac{16\Psi^2}{3V_0}\right)^{\frac{1}{n}}. \tag{41}$$

4.1 Weak dissipative regime ($Q \ll 1$)

For weak dissipative regime, Eq. (24) can be written as

$$\dot{\phi} = -\frac{V'(\phi)}{3H} \tag{42}$$

which on integration gives

$$\phi = \phi_0 t^{\frac{2}{4-n}} \tag{43}$$

where $\phi_0^{\frac{4-n}{2}} = \frac{n(n-4)}{2}\sqrt{\frac{V_0}{3}}$. The Hubble parameter can be written as

$$H(\phi) = \sqrt{\frac{V_0}{3}}\phi^{\frac{n}{2}} \tag{44}$$

The first two slow-roll parameters can be written as

$$\epsilon_1(\phi) = \frac{n^2}{2\phi^2},\ \eta(\phi) = \frac{n(n-1)}{\phi^2} \tag{45}$$

At the end of inflation, $\epsilon_1(\phi_e) = 1$. Therefore, $\phi_e^2 = \frac{n^2}{2}$. The number of e-folds is given by

$$N = -\int_{\phi_\star}^{\phi_e} \frac{V}{V'}d\phi = \frac{1}{2n}\left[\phi_\star^2 - \frac{n^2}{2}\right] \tag{46}$$

which leads to the expression for the scalar field at the horizon crossing time given by

$$\phi_\star^2 = \frac{n^2}{2}\left[1 + \frac{4N}{n}\right]. \tag{47}$$

Hence it follows that the slow-roll parameters at the horizon crossing time can be written as

$$\epsilon_{1_\star} = \left(1 + \frac{4N}{n}\right)^{-1},\quad \eta_\star = \frac{2(n-1)}{n}\epsilon_{1_*}. \tag{48}$$

Now, to study further for spectral index we have to choose some particular form of the dissipation coefficient as follows: (i) $\Gamma = \Gamma_0\phi^m$, (ii) $\Gamma = \Gamma_0 T^m$ and (iii) $\Gamma = \Gamma_0\frac{T^m}{\phi^{m-1}}$.

The other slow-roll parameter β at the horizon crossing time for these three choices of Γ can be written as

$$\beta_\star = \begin{cases} \frac{2m}{n}\epsilon_{1_\star} & \text{for } \Gamma = \Gamma_0\phi^m \\ \frac{m(n-4)}{n(4-m)}\epsilon_{1_\star} & \text{for } \Gamma = \Gamma_0 T^m \\ \frac{(12m - mn - 8)}{n(m-4)}\epsilon_{1_\star} & \text{for } \Gamma = \Gamma_0\frac{T^m}{\phi^{m-1}} \end{cases} \tag{49}$$

Here one may note that for each choice of Γ, temperature T can be explicitly written as a function of the inflaton field ϕ. So the dissipation coefficient remains no longer function of (ϕ, T), it becomes a function of ϕ only. The expressions

for temperature can be written as

$$T=\begin{cases}\left(\frac{\Gamma_0 n^2}{4C_\gamma}\sqrt{\frac{V_0}{3}}\right)^{\frac{1}{4}}\phi^{\frac{2m+n-4}{8}} & \text{for } \Gamma=\Gamma_0\phi^m\\ \left(\frac{\Gamma_0 n^2}{4C_\gamma}\sqrt{\frac{V_0}{3}}\right)^{\frac{1}{4-m}}\phi^{\frac{n-4}{2(4-m)}} & \text{for } \Gamma=\Gamma_0 T^m\\ \left(\frac{\Gamma_0 n^2}{4C_\gamma}\sqrt{\frac{V_0}{3}}\right)^{\frac{1}{4-m}}\phi^{\frac{2m-n+2}{2(m-4)}} & \text{for } \Gamma=\Gamma_0\frac{T^m}{\phi^{m-1}}\end{cases} \tag{50}$$

Substituting the values of the slow-roll parameters, the spectral index at the horizon crossing time can be written in terms of no. of e-folds as

$$n_{s_\star}(n,m,N)=\begin{cases}1-\frac{5n+2m+12}{4n}\left(1+\frac{4N}{n}\right)^{-1} & \text{for } \Gamma=\Gamma_0\phi^m\\ 1-\frac{(5n-4m-mn+12)}{n(4-m)}\left(1+\frac{4N}{n}\right)^{-1} & \text{for } \Gamma=\Gamma_0 T^m\\ 1-\frac{(mn-5n+6m-14)}{n(m-4)}\left(1+\frac{4N}{n}\right)^{-1} & \text{for } \Gamma=\Gamma_0\frac{T^m}{\phi^{m-1}}\end{cases} \tag{51}$$

The tensor-to-scalar ratio at the horizon crossing time can be written as

$$r_\star(n,m,N)=\begin{cases}16\left(\frac{2C_\gamma}{\Gamma_0}\right)^{\frac{1}{4}}\left(\frac{V_0}{3}\right)^{\frac{3}{8}}\left(\frac{n^2}{2}\right)^{\frac{3n-2m}{16}}\left(1+\frac{4N}{n}\right)^{\frac{3n-2m-12}{16}} & \text{for } \Gamma=\Gamma_0\phi^m\\ 16\left(\frac{2C_\gamma}{\Gamma_0}\right)^{\frac{1}{4-m}}\left(\frac{V_0}{3}\right)^{\frac{3-m}{2(4-m)}}\left(\frac{n^2}{2}\right)^{\frac{n(3-m)}{4(4-m)}}\left(1+\frac{4N}{n}\right)^{\frac{(m-3)(n-4)}{4(m-4)}} & \text{for } \Gamma=\Gamma_0 T^m\\ 16\left(\frac{2C_\gamma}{\Gamma_0}\right)^{\frac{1}{4-m}}\left(\frac{V_0}{3}\right)^{\frac{3-m}{2(4-m)}}\left(\frac{n^2}{2}\right)^{\frac{mn-3n-2m+2}{4(m-4)}}\left(1+\frac{4N}{n}\right)^{\frac{mn-3n-6m+14}{4(m-4)}} & \text{for } \Gamma=\Gamma_0\frac{T^m}{\phi^{m-1}}\end{cases} \tag{52}$$

However, using the definition of P_s, the tensor-to-scalar ratio at the same time for all the choices of Γ in weak dissipative regime can be written as

$$r_*(n,m,N)=\frac{8V_0}{3P_{s_\star}(n,m,N)}\left\{\frac{n^2}{2}\left(1+\frac{4N}{n}\right)\right\}^{\frac{n}{2}} \tag{53}$$

where the amplitude of the scalar perturbation P_s at the horizon crossing time for the above three choices of Γ is given by

$$P_{s_\star}(n,m,N)=\begin{cases}\frac{1}{2}\left(\frac{\Gamma_0}{2C_\gamma}\right)^{\frac{1}{4}}\left(\frac{V_0}{3}\right)^{\frac{5}{8}}\left(\frac{n^2}{2}\right)^{\frac{2m+5n}{16}}\left(1+\frac{4N}{n}\right)^{\frac{2m+5n+12}{16}} & \text{for } \Gamma=\Gamma_0\phi^m\\ \frac{1}{2}\left(\frac{\Gamma_0}{2C_\gamma}\right)^{\frac{1}{4-m}}\left(\frac{V_0}{3}\right)^{\frac{5-m}{2(4-m)}}\left(\frac{n^2}{2}\right)^{\frac{n(5-m)}{4(4-m)}}\left(1+\frac{4N}{n}\right)^{\frac{mn+4m-12-5n}{4(m-4)}} & \text{for } \Gamma=\Gamma_0 T^m\\ \frac{1}{2}\left(\frac{\Gamma_0}{2C_\gamma}\right)^{\frac{1}{4-m}}\left(\frac{V_0}{3}\right)^{\frac{5-m}{2(4-m)}}\left(\frac{n^2}{2}\right)^{\frac{mn-5n+2m-2}{4(m-4)}}\left(1+\frac{4N}{n}\right)^{\frac{mn-5n+6m-14}{4(m-4)}} & \text{for } \Gamma=\Gamma_0\frac{T^m}{\phi^{m-1}}\end{cases} \tag{54}$$

Now, during inflation, the first slow-roll parameter ϵ_1 evolves from a very small positive value and increases till the end of inflation i.e., $N\sim 55-60$. Hence $n\lesssim -220$. Therefore, though one can consider WDR in torsion gravity for power law potential theoretically, physically it is very unrealistic due to very small values of potential. Using the $r-n_s$ diagram of Planck-2018, one could plot a $n-m$ diagram as shown in Fig. 1, where the dark blue colour and light blue colour indicate an area of (n,m) in which the point (r,n_s) of the model stand in the observationally favored region.

4.2 Strong dissipative regime

For strong dissipative regime, Eq. (24) can be written as

$$\dot\phi=-\frac{V'(\phi)}{\Gamma} \tag{55}$$

So one may note that it is necessary to choose a form of dissipation coefficient Γ from the very beginning stage, to study the SDR in torsion gravity. Similar to WDR, here also same choices of Γ have been considered.

4.2.1 $\Gamma=\Gamma_0\phi^m$

Substituting the choice of Γ, expression for scalar field can be written as

$$\phi=\phi_0 t^{\frac{1}{m-n+2}} \tag{56}$$

where $\phi_0=\left[\frac{n(n-m-2)V_0}{\Gamma_0}\right]^{\frac{1}{m-n+2}}$. As the Hubble parameter directly depends on the potential $V(\phi)$, the expression for the Hubble parameter is same for both WDR & SDR and it is given by

$$H=\sqrt{\frac{V_0}{3}}\phi^{\frac{n}{2}} \tag{57}$$

The slow-roll parameters can be written as

$$\epsilon_1=\frac{\sqrt{3V_0}n^2}{2\Gamma_0}\phi^{\frac{n-2m-4}{2}},\ \eta=\frac{2(n-1)}{n}\epsilon_1,\ \beta=\frac{2m}{n}\epsilon_1. \tag{58}$$

Now, inflation ends when $\epsilon_1(\phi_e)=1$ which gives $\phi^{\frac{2m-n+4}{2}}=\frac{\sqrt{3V_0}n^2}{2\Gamma_0}$. Using this relation, no. of e-folds N

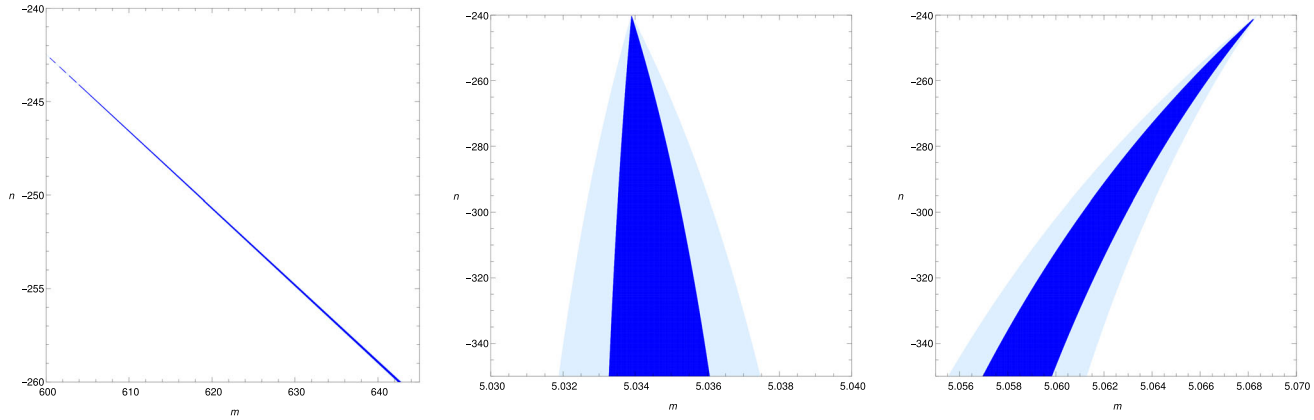

Fig. 1 Numerical values of the (n, m) parameters of the torsion warm inflation models namely (left: $\Gamma = \Gamma_0\phi^m$, center: $\Gamma = \Gamma_0 T^m$, right: $\Gamma = \Gamma_0 \frac{T^m}{\phi^{m-1}}$) in the weak dissipative regime for which the point $(r - n_s)$ is located in the observational region

can be written as

$$N = \frac{1}{n(2m-n+4)}\left[\frac{2\Gamma_0}{\sqrt{3V_0}}\phi_\star^{\frac{2m-n+4}{2}} - n^2\right] \tag{59}$$

and the scalar field at the horizon crossing time, $\phi_\star$ is given by

$$\phi_\star^{\frac{2m-n+4}{2}} = \frac{\sqrt{3V_0}n^2}{2\Gamma_0}\left[1 + \frac{(2m-n+4)}{n}N\right]. \tag{60}$$

The slow-roll parameters at that time is given by

$$\epsilon_{1_\star} = \left[1 + \frac{(2m-n+4)}{n}N\right]^{-1}, \ \eta = \frac{2(n-1)}{n}\epsilon_{1_\star}, \quad \beta = \frac{2m}{n}\epsilon_{1_\star}. \tag{61}$$

The scalar spectral index at the horizon crossing time is obtained as

$$n_{s_\star}(n, m, N) = 1 - \frac{3}{4n}(6m-n+4) \times \left[1 + \frac{(2m-n+4)}{n}N\right]^{-1} \tag{62}$$

The tensor-to-scalar ratio at the horizon crossing time can explicitly be written as

$$r_\star = 16\frac{3\sqrt{2}C_\gamma^{\frac{1}{4}}}{\Gamma_0^{\frac{5}{4}}}\sqrt{\frac{2}{n}}\left(\frac{V_0}{3}\right)^{\frac{5}{8}}\phi_\star^{\frac{7n-10m+4}{8}} \tag{63}$$

where $\phi_\star$ is given by Eq. (60). Using the definition of amplitude of the power spectrum P_s, it can be simplified in terms of no. of e-folds as

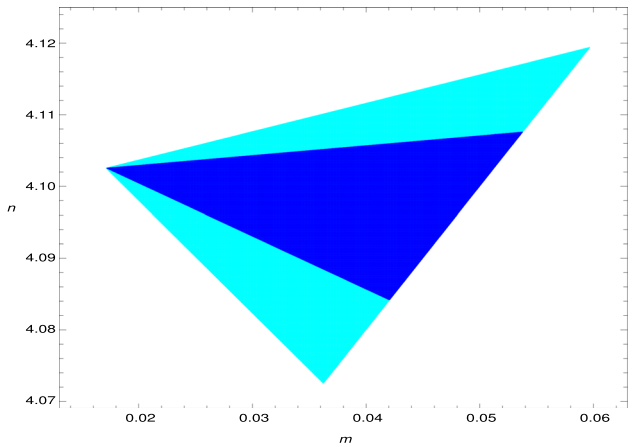

Fig. 2 In the strong dissipative regime of the torsion warm inflationary model with $\Gamma = \Gamma_0\phi^m$ the observed region in the figure indicates the location of the (n,m) points by using the precise values of (r, n_s) parameters as favored by the Planck 2018 data set [35]

$$r_\star(n, m, N) = \frac{8V_0}{3P_{s_\star}(n, m, N)}\left\{\frac{\sqrt{3V_0}n^2}{2\Gamma_0} \times \left[1 + \frac{(2m-n+4)}{n}N\right]\right\}^{\frac{2n}{2m-n+4}} \tag{64}$$

In Fig. 2 at 68% and 95% CL, the points (r, n_s) of the model are indicated by dark blue colour and light blue colour respectively in the $n-m$ plot, considering $r-n_s$ diagram of Planck 2018 data. Choosing some points of (n, m) from Fig. 2, the evolution of the slow-roll parameters with respect to the number of e-folds have been plotted in Fig. 3 and it matches with the slow-roll approximations. The behaviour of n_s and r have been represented in Fig. 4. The Figs. 3 and 4 have been drawn considering the values for (n, m) as (4.102, 0.02) (red solid line), (4.101, 0.025) (blue dotted line) and (4.1, 0.03) (brown dot-dashed line).

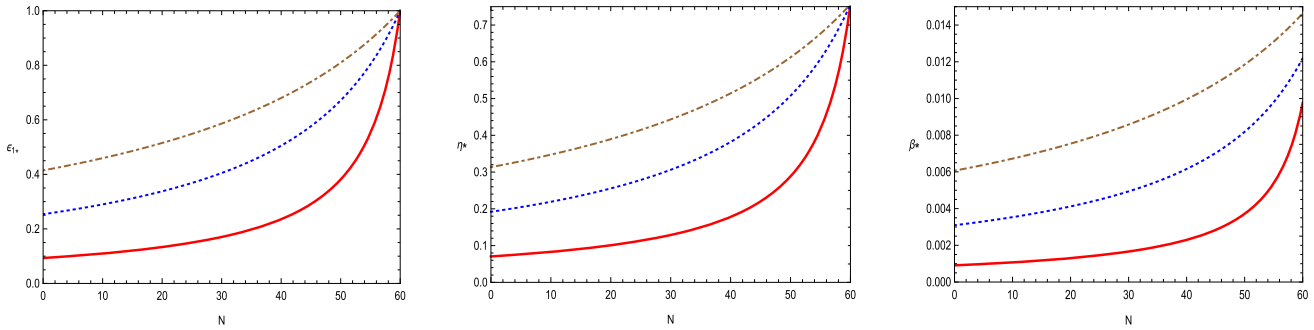

Fig. 3 Variation of slow-roll parameters namely (ϵ_{1*}, $\eta*$, $\beta*$) with number of e-folds (N)

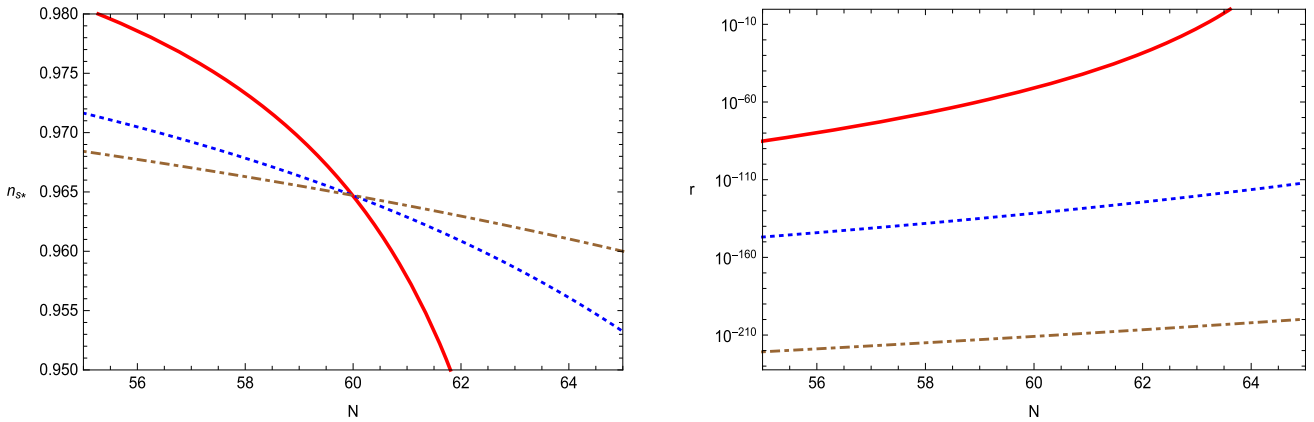

Fig. 4 Spectral index (n_s*) and tensor-to-scalar ratio (r) vs number of e-folds (N)

4.2.2 $\Gamma = \Gamma_0 \mathbf{T^m}$

The evolution of the temperature is given by

$$T = T_0 \phi^{\frac{(3n-4)}{2(m+4)}} \tag{65}$$

with T_0, given by $T_0^{m+4} = \dfrac{n^2 V_0^2}{4C_\gamma \Gamma_0}\sqrt{\dfrac{3}{V_0}}$. As a consequence, the dissipation coefficient reduces to a function of ϕ only.

The slow-roll parameters can be written as

$$\epsilon_1 = \frac{\sqrt{3V_0}n^2}{2\Gamma_0 T_0^m}\phi^{\frac{2n-mn-8}{m+4}},\ \eta = \frac{2(n-1)}{n}\epsilon_1,$$
$$\beta = \frac{m(3n-4)}{n(m+4)}\epsilon_1. \tag{66}$$

Now, inflation ends when $\epsilon_1(\phi_e) = 1$ which leads to $\phi^{\frac{mn-2n+8}{m+4}} = \dfrac{\sqrt{3V_0}n^2}{2\Gamma_0 T_0^m}$. Using this relation, no. of e-folds N can be written as

$$N = \frac{m+4}{mn-2n+8}\left[\frac{\Gamma_0 T_0^m}{\sqrt{3V_0}n}\phi_\star^{\frac{mn-2n+8}{m+4}} - \frac{n}{2}\right] \tag{67}$$

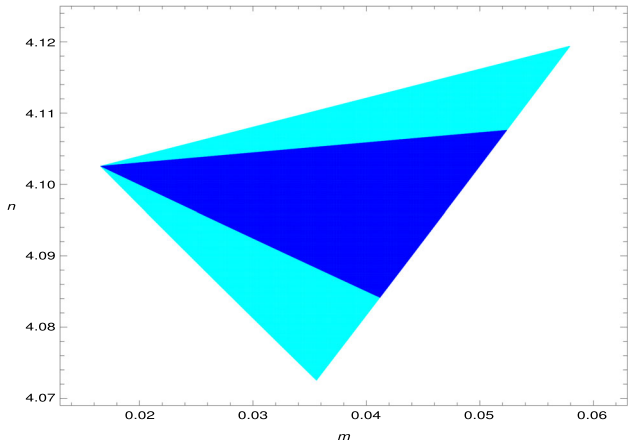

Fig. 5 In the strong dissipative regime of the torsion warm inflationary model with $\Gamma = \Gamma_0 T^m$, the observed region in the figure indicates the location of the (n,m) points by using the precise values of (r, n_s) parameters as favored by Planck 2018 data set [35]

and the scalar field at the horizon crossing time, $\phi_\star$ is given by

$$\phi_\star^{\frac{mn-2n+8}{m+4}} = \frac{\sqrt{3V_0}n^2}{2\Gamma_0 T_0^m}\left[1 + \frac{2}{n}\frac{(mn-2n+8)}{(m+4)}N\right] \tag{68}$$

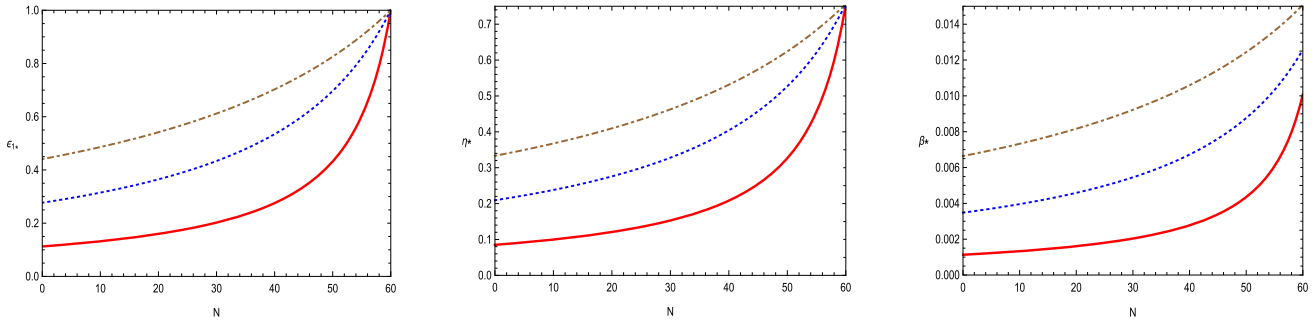

Fig. 6 Variation of slow-roll parameters namely (ϵ_1*, $\eta*$, $\beta*$) with number of e-folds (N)

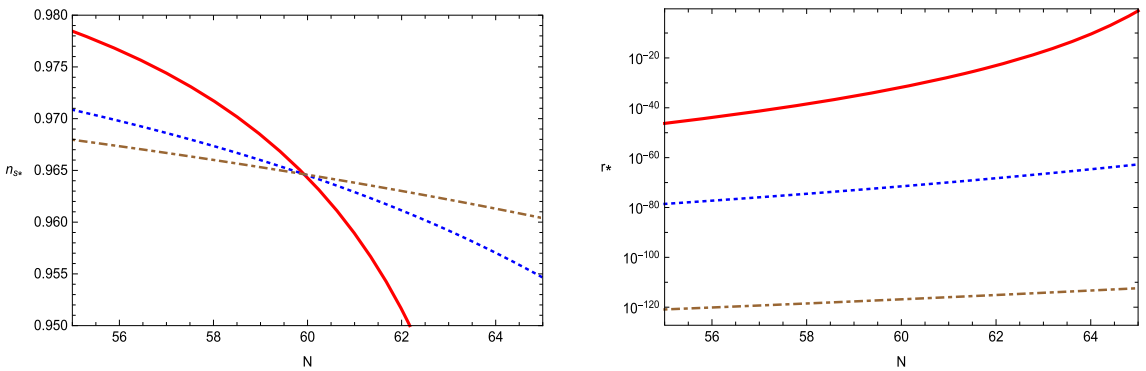

Fig. 7 Spectral index (n_s*) and tensor-to-scalar ratio (r_*) vs number of e-folds (N)

slow-roll parameters at the horizon crossing time are given by:

$$\epsilon_{1_\star} = \left[1 + \frac{2}{n}\frac{(mn-2n+8)}{(m+4)}N\right]^{-1}, \quad \eta_\star = \frac{2(n-1)}{n}\epsilon_{1_\star},$$
$$\beta_\star = \frac{m(3n-4)}{n(m+4)}\epsilon_{1_\star} \tag{69}$$

Expression for scalar spectral index is given by

$$n_{s_\star}(n,m,N) = 1 - \frac{3}{n}\frac{(2mn-n-2m+4)}{(m+4)} \times \left[1 + \frac{2}{n}\frac{(mn-2n+8)}{(m+4)}N\right]^{-1} \tag{70}$$

The tensor-to-scalar ratio at the horizon crossing time can explicitly be written as

$$r_\star = 16\frac{3^{\frac{8-3m}{2(m+4)}}C_\gamma^{\frac{3m+2}{2(m+4)}}}{\Gamma_0^{\frac{5}{4+m}}}\left(\frac{2}{n}\right)^{\frac{3m+2}{m+4}}\left(\frac{V_0}{3}\right)^{\frac{7-2m}{2(m+4)}}\phi_\star^{\frac{6m+7n-2mn+4}{2(m+4)}} \tag{71}$$

where $\phi_\star$ is given by Eq. (68). Using the definition of amplitude of the power spectrum P_s, it can be simplified in terms of no. of e-folds as

$$r_\star(n,m,N) = \frac{8V_0}{3P_{s_\star}(n,m,N)}\left\{\frac{\sqrt{3V_0}n^2}{2\Gamma_0 T_0^m} \times \left[1 + \frac{2}{n}\frac{(mn-2n+8)}{(m+4)}N\right]\right\}^{\frac{2(m+4)}{mn-2n+8}} \tag{72}$$

In Fig. 5 at 68% and 95% CL, the points (r, n_s) of the model are indicated by dark blue colour and light blue colour respectively in the $n-m$ plot, considering $r-n_s$ diagram of Planck 2018 data. Choosing some points of (n, m) from Fig. 5, the evolution of the slow-roll parameters with respect to the number of e-folds have been plotted in Fig. 6 and it matches with the slow-roll approximations. The behavior of n_s and r have been represented in Fig. 7. The Figs. 6 and 7 have been drawn considering the values for (n, m) as (4.102, 0.02) (red solid line), (4.101, 0.025) (blue dotted line) and (4.1, 0.03) (brown dot-dashed line).

4.2.3 $\Gamma = \Gamma_0 \frac{\mathbf{T^m}}{\phi^{\mathbf{m-1}}}$

The evolution of the temperature is obtained as

$$T = T_0\phi^{\frac{(2m+3n-6)}{2(m+4)}} \tag{73}$$

Using the above relation, the dissipation coefficient can be reduced to a function of ϕ alone similar to the previous case. The slow-roll parameters can be written as

$$\epsilon_1 = \frac{\sqrt{3V_0}n^2}{2\Gamma_0 T_0^m}\phi^{\frac{2n+4m-mn-12}{m+4}}, \quad \eta = \frac{2(n-1)}{n}\epsilon_1,$$

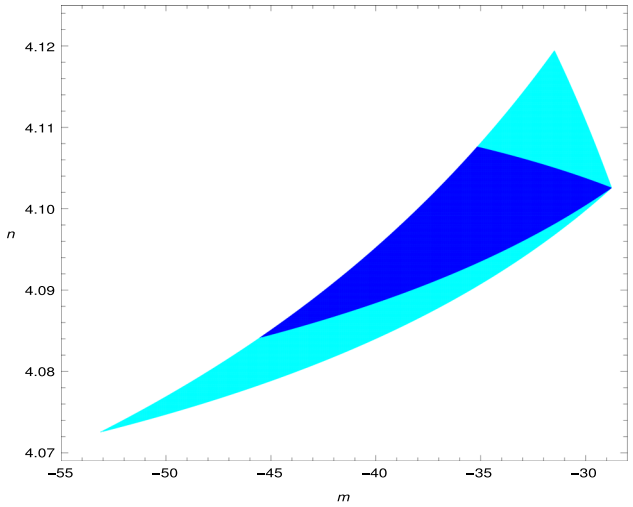

Fig. 8 In the strong dissipative regime of the torsion warm inflationary model with $\Gamma = \Gamma_0 \frac{T^m}{\phi^{m-1}}$, the observed region in the figure indicates the location of the (n,m) points by using the precise values of (r, n_s) parameters as favored by Planck 2018 data set

$$\beta = \frac{(3mn - 12m + 8)}{n(m+4)}\epsilon_1. \tag{74}$$

Now, inflation ends when $\epsilon_1(\phi_e) = 1$ which gives $\phi^{\frac{mn-2n-4m+12}{m+4}} = \frac{\sqrt{3V_0}n^2}{2\Gamma_0 T_0^m}$. Using this relation, no. of e-folds N can be written as

$$N = \frac{m+4}{mn-2n-4m+12}\left[\frac{\Gamma_0 T_0^m}{\sqrt{3V_0}n}\phi_\star^{\frac{mn-2n-4m+12}{m+4}} - \frac{n}{2}\right] \tag{75}$$

and the scalar field at the horizon crossing time, $\phi_\star$ is given by

$$\phi_\star^{\frac{mn-2n-4m+12}{m+4}} = \frac{\sqrt{3V_0}n^2}{2\Gamma_0 T_0^m}\left[1 + \frac{2}{n}\frac{(mn-2n-4m+12)}{(m+4)}N\right] \tag{76}$$

slow-roll parameters at the horizon crossing time are given by:

$$\epsilon_{1_\star} = \left[1 + \frac{2}{n}\frac{(mn-2n-4m+12)}{(m+4)}N\right]^{-1},$$
$$\eta_\star = \frac{2(n-1)}{n}\epsilon_{1_\star},\ \beta_\star = \frac{(3mn-12m+8)}{n(m+4)}\epsilon_{1_\star} \tag{77}$$

Expression for scalar spectral index at that time is given by

$$n_{s_\star}(n,m,N) = 1 - \frac{3}{n}\frac{(2mn-n-8m+10)}{(m+4)} \times \left[1 + \frac{2}{n}\frac{(mn-2n-4m+12)}{(m+4)}N\right]^{-1}. \tag{78}$$

The tensor-to-scalar ratio at the horizon crossing time can explicitly be written as

$$r_\star = 16\frac{3^{\frac{8-3m}{2(m+4)}}C_\gamma^{\frac{3m+2}{2(m+4)}}}{\Gamma_0^{\frac{5}{4+m}}}\left(\frac{2}{n}\right)^{\frac{3m+2}{m+4}}\left(\frac{V_0}{3}\right)^{\frac{7-2m}{2(m+4)}}\phi_\star^{\frac{16m+7n-2mn-6}{2(m+4)}}, \tag{79}$$

where $\phi_\star$ is given by Eq. (68). Using the definition of amplitude of the power spectrum P_s, it can be simplified in terms of no. of e-folds as

$$r_\star(n,m,N) = \frac{8V_0}{3P_{s_\star}(n,m,N)}\left\{\frac{\sqrt{3V_0}n^2}{2\Gamma_0 T_0^m} \times \left[1 + \frac{2}{n}\frac{(mn-2n-4m+12)}{(m+4)}N\right]\right\}^{\frac{2(m+4)}{mn-2n-4m+12}}. \tag{80}$$

One may note that Eq. (73) reduces Γ in this case (i.e $\Gamma = \Gamma_0 \frac{T^m}{\phi^{m-1}}$) to a function of ϕ alone with some modified powers and coefficients. Hence study of graphs (showing the variation of slow-roll parameters, spectral index and tensor-to-scalar ratio w.r.t no. of e-folds) is not repeated in this section. Figure 8 indicates the location of (n,m) points in the observational region for the strong dissipative regime case of the present torsion warm inflationary model $\Gamma = \Gamma_0 \frac{T^m}{\phi^{m-1}}$, considering the numerical values of (r, n_s) parameters from Planck 2018 data set.

5 Numerical analysis and observational constraint

We can see here that spectral index n_s is a function of the (i) dissipative coefficient Γ_0, (ii) quartic coupling constant (V_0) of the inflaton potential, (iii) the polynomial power of the potential (n) and (iv) the power of the dissipation factor (m). Apart from these primordial parameters, we also consider baryonic matter density $\omega_b = \Omega_b h^2$ and cold dark matter density $\omega_{cdm} = \Omega_{cdm} h^2$ components, where $h = H_0 100^{-1}$, H_0 is the present Hubble parameter to consider spatially flat background cosmological model. Now to constrain the model parameters we analyze the observational data sets. In order to do so, we have modified the public version of the CLASS Boltzmann code. The MCMC code Montepython3.5 [38] has been used to estimate the relevant cosmological parameters. In order to analyze, we use the cosmological datasets (Pantheon [4], BAO (BOSS DR12 [39], *SMALLZ*-2014 [40]) and HST [41]) and a PLANCK18 prior has been imposed. We

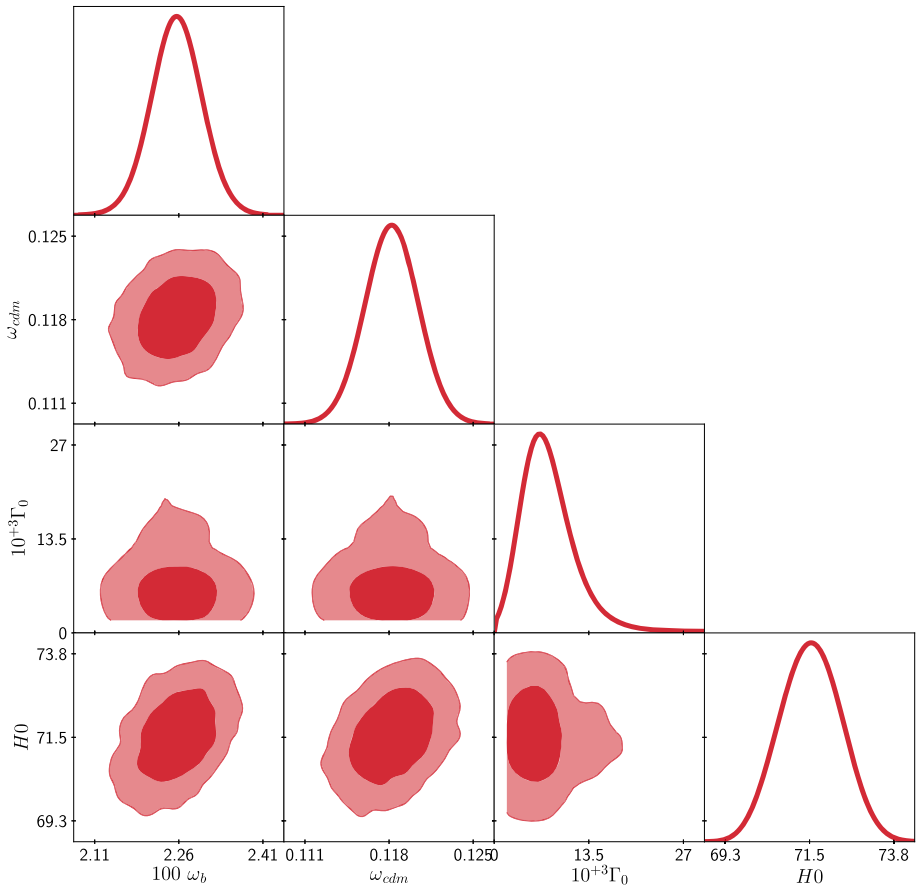

Fig. 9 Posterior distribution for the cosmological parameters for the choice ($\Gamma = \Gamma_0 T^m,\ m = 1$) using data set (Pantheon +BAO + HST) and PLANCK18 prior has been considered

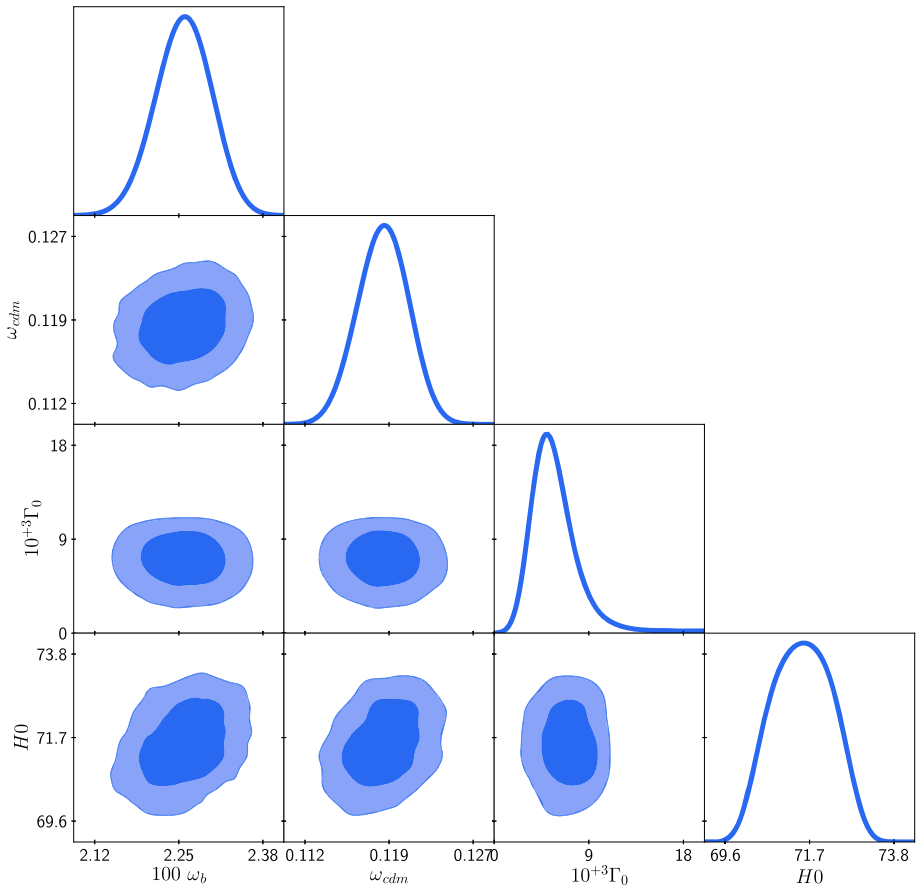

Fig. 10 Posterior distribution for the cosmological parameters for the choice $\Gamma = \Gamma_0 \frac{T^m}{\phi^{m-1}}$, $(m = -1)$ using data set (Pantheon +BAO + HST) and PLANCK18 prior has been considered

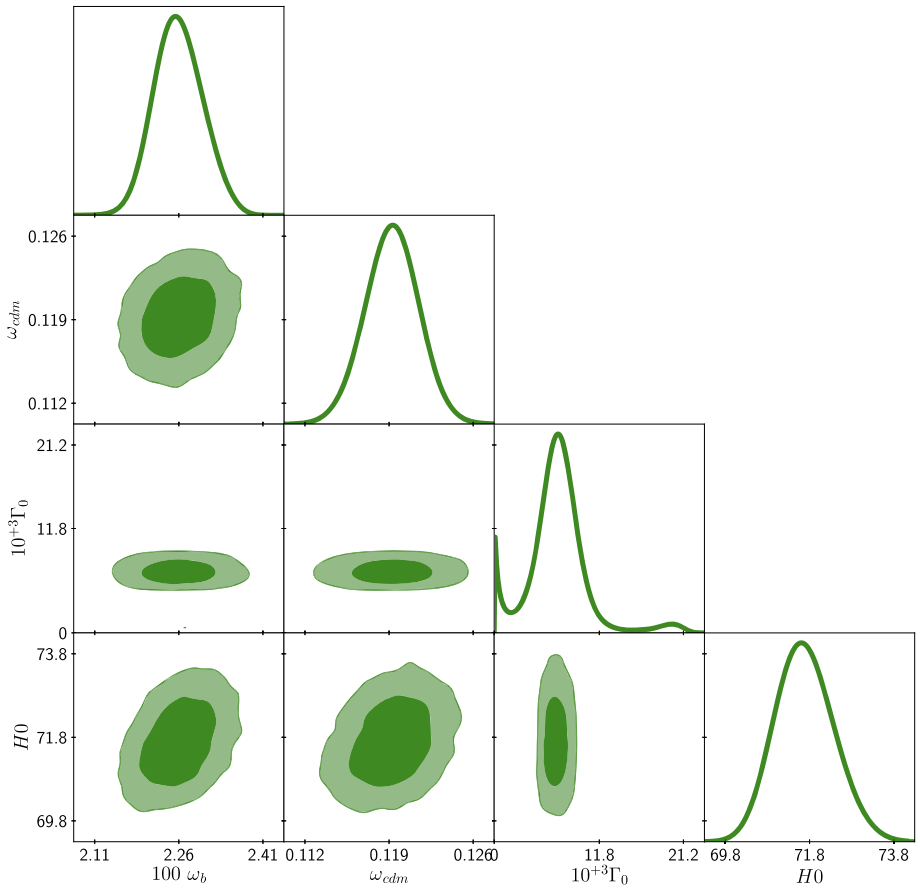

Fig. 11 Posterior distribution for the cosmological parameters for the choice $\Gamma = \Gamma_0 \frac{T^m}{\phi^{m-1}}$, $m = 2$ using data set (Pantheon +BAO + HST) and PLANCK18 prior has been considered

Table 1 $\Gamma = \Gamma_0 T^m, m = 1\ \chi^2_{min} = 1035$

Param	Best-fit	Mean$\pm\sigma$
$100\ \omega_b$	2.251	$2.257^{+0.047}_{-0.046}$
ω_{cdm}	0.1185	$0.1187^{+0.0023}_{-0.0022}$
$10^{+3}\Gamma_0$	6.89	$7.717^{+0.12}_{-4.3}$
$H0$	71.42	$71.56^{+0.82}_{-0.84}$

Table 2 $\Gamma = \Gamma_0 \frac{T^m}{\phi^{m-1}}, (m = -1), \chi^2_{min} = 1035$

Param	Best-fit	Mean$\pm\sigma$
$100\ \omega_b$	2.246	$2.255^{+0.046}_{-0.043}$
ω_{cdm}	0.1186	$0.1186^{+0.0023}_{-0.0021}$
$10^{+3}\Gamma_0$	7.351	$7.113^{+1.8}_{-1.7}$
$H0$	71.47	$71.51^{+0.67}_{-0.81}$

Table 3 $\Gamma = \Gamma_0 \frac{T^m}{\phi^{m-1}}, (m = 2), \chi^2_{min} = 1035$

Param	Best-fit	Mean$\pm\sigma$
$100\ \omega_b$	2.255	$2.261^{+0.046}_{-0.045}$
ω_{cdm}	0.1183	$0.1188^{+0.0023}_{-0.0022}$
$10^{+3}\Gamma_0$	6.901	$6.948^{+0.75}_{-0.98}$
$H0$	71.43	$71.69^{+0.71}_{-0.77}$

have made the choice of flat priors on the base cosmological parameters as follows: the baryon density $100\omega_b = [1.9, 2.5]$; cold dark matter density $\omega_{cdm} = [0.0, 0.145]$; Hubble parameter $H_0 = [60, 80]\text{km s}^{-1}Mpc^{-1}$ and a wide range of flat prior has been chosen for $10^3\Gamma_0 = [0, 30]$. Besides, we have made a choice of $n = 4$ (for quartic potential), $V_0 = 10^{-15}$, $n_s = 0.9649$ (taken from Planck data [35]), $m = -1, 1, 2$ for different dissipative models. The posterior distribution for the cosmological parameters are given in Figs. 9, 10 and 11 for three different choices of Γ using this data set and the corresponding constraints are enlisted in Tables 1, 2 and 3.

For warm inflation without torsion, $\Gamma_0 = 0.0104$ (using Planck 2015 data and BICEP2/Keck array data) [31] in case of $m = 1$ or the model $\Gamma = \Gamma_0 T$ whereas in this case (i.e, warm inflation with torsion) $\Gamma_0 = 0.00689$ (Table 1). Further, the tensor-to-scalar ratio r in this model is 1.435×10^{-3} which is supported by the Planck 2018 data. For the model $\Gamma = \Gamma_0 \frac{T^m}{\phi^{m-1}}; m = -1$ the tensor-to-scalar ratio is $r = 0.12 \times 10^{-11}$ which is also corroborated by the Planck 2018 data. However, for $m = 2$, $r = 1.96$ and hence the

model is disproved by the Planck 2018 data. Thus the models $\Gamma = \Gamma_0 T$ and $\Gamma = \Gamma_0 \frac{\phi^2}{T}$ support warm inflation as per recent observational evidence while the model $\Gamma = \Gamma_0 \frac{T^2}{\phi}$ is a worse fit to describe warm inflationary scenario.

6 Summary and conclusion

A detailed study of WI has been done in the background of flat FLRW model with torsion. The interaction term between the inflaton field and the radiation field are considered for the three possible choices namely (1) $\Gamma = \Gamma_0 \phi^m$ (ϕ is the inflaton field), (2) $\Gamma = \Gamma_0 T^m$ (T is the temperature of the radiation bath) and (3) $\Gamma = \Gamma_0 \frac{T^m}{\phi^{m-1}}$ (m, constant). The slow-roll parameters, number of e-folds, the spectral index and tensor-to-scalar ratio are evaluated for the above three choices. In the underlying model due to quasi-stable conditions and the slow-roll approximation the Hubble parameter is approximated linearly to the torsion function. The potential of the scalar field is chosen in power-law form and it is found that the scalar field (inflaton) can be expressed as some power of the torsion function. In the present context the usual fluid is considered as inflaton and the effective fluid as radiation so that the study is consistent with quasi stable condition and slow-roll approximations and with this choice of fields we have observed that energy is transferred from the scalar field to the radiation fluid during WI. Since the scalar field varies approximately with some power of the torsion function therefore effect of torsion in WI comes through the scalar field. Subsequently the study is carried out both in the weak and strong dissipative regimes.

It is shown that in WDR, the scalar field, Hubble parameter (and hence scale factor), no. of e-folds and the first two slow-roll parameters can be expressed explicitly without choosing the dissipation coefficient. However to determine the temperature (T), third slow-roll parameter, spectral index and scalar to tensor ratio choices for Γ need to be considered. The choice $\Gamma = \Gamma_0 \phi^m$ expresses the scalar spectral index and tensor-to-scalar ratio in terms of the model parameters (n, m). The feasible range for (n, m) has been found using the $r - n_s$ diagram of Planck-2018 data set. The variations of the slow-roll parameters with no.of e-folds has been studied graphically and the results are compatible with the slow-roll approximations. Similar analysis has been done for the choice $\Gamma = \Gamma_0 T^m$. The third choice of Γ although involves both ϕ and T but the evolution of temperature shows that Γ is a function of ϕ alone and hence reduces to the first case. Since in SDR, $\Gamma >> 3H$ (dissipative coefficient predominates over the Hubble parameter), one needs the choices for Γ at every step. Further in this regime variation of slow-roll parameters, spectral index and tensor-to-scalar ratio has been studied graphically and they are found to be consistent with suitable choice of the model parameters.

Finally by considering single-field chaotic quartic potential i.e. $V = V_0 \phi^4$, where $V_0 = 10^{-15}$ we have analyzed Γ for three different choices namely ((1) $\Gamma = \Gamma_0 T$, (2) $\Gamma = \Gamma_0 \frac{\phi^2}{T}$ and (3) $\Gamma = \Gamma_0 \frac{T^2}{\phi}$) using the data set (Pantheon+ BAO+ HST) with Planck 18 prior. The observational study reveals that the best fit value for Γ_0 is almost same for the models $\Gamma = \Gamma_0 T$ and $\Gamma = \Gamma_0 \frac{T^2}{\phi}$. In case of the linear model $\Gamma = \Gamma_0 T$, $\Gamma_0 = 0.0104$ for warm inflation without torsion (using Planck 2015 data and BICEP2/Keck array data) [31] whereas in the present work (i.e, warm inflation with torsion) $\Gamma_0 = 0.00689$ (Table 1). The value of r (tensor-to-scalar ratio) for the three models show that the models (1) and (2) are successful to describe warm inflationary scenario as per Planck 2018 data while the model (3) is a worst fit in this context. Further we have evaluated first slow-roll parameter (ϵ_1) in terms of the inflaton (ϕ) in the three cases as $6.7 \times \phi^{-0.8}$, $6.3 \times \phi^{-4}$ and $7 \times 10^5 \times \phi^{-0.67}$ respectively which shows that the first two models show similar behavior towards inflation.

Acknowledgements The authors M.C. and A.B. thank University Grant Commission (UGC) for providing their respective Junior (ID: 211610035684/JOINTCSIR-UGCNETJUNE2021) and Senior (ID: 1207/CSIRNETJUNE2019) Research Fellowship. Author G.S. acknowledges UGC for Dr. D.S. Kothari Postdoctoral Fellowship (No.F.4-2/2006 (BSR)/PH/19-20/0104). S.C. thanks FIST program of DST (SR/FST/MS-II/2021/101(C)).

Data Availability Statement The manuscript has associated data in a data repository. [Authors' comment: The datasets used in this work to constrain the models are public data available in their respective references].

Funded by SCOAP^3. SCOAP^3 supports the goals of the International Year of Basic Sciences for Sustainable Development.

Appendix

If the usual fluid is considered as radiation fluid and the effective fluid is assumed to be inflaton, i.e., $\rho = \rho_r$, $p = p_r$.

$\rho_f = \rho_\phi = \frac{1}{2}\dot{\phi}^2 + V(\phi)$, $p_f = p_\phi = \frac{1}{2}\dot{\phi}^2 - V(\phi)$, then the evolution of the two fluid can be written as

$$\dot{\rho}_r + 3(H + 2\Psi)(\rho_r + p_r) = 4\Psi\rho_r \tag{81}$$

$$\text{i.e.,} \quad \dot{\rho}_r + 4H\rho_r = -4\Psi\rho_r = \Gamma\dot{\phi}^2 \tag{82}$$

$$\text{and} \quad \dot{\rho}_\phi + 3H(\rho_\phi + p_\phi) = 4\Psi\rho_r = -\Gamma\dot{\phi}^2 \tag{83}$$

Now assuming the quasi-stable production of the radiation fluid i.e. $\dot{\rho}_r \ll 4H\rho_r, \Gamma\dot{\phi}^2$, one have

$$H \simeq -\Psi$$

Using this condition one can simplify the energy density of the inflaton field ρ_ϕ as

$$\rho_\phi = -12\Psi^2 - 12H\Psi \simeq 0$$

which is inconsistent with the slow-roll approximation that $\rho_\phi >> \rho_r$. So for the warm inflation in torsion gravity, the slow-roll conditions and the quasi-stable condition cannot hold simultaneously if one consider the usual fluid as radiation and the effective fluid as inflaton.

References

1. N. Aghanim et al., [Planck], Astron. Astrophys. **641**, A6 (2020)
2. C.L. Bennett et al., [WMAP], Astrophys. J. Suppl. **208**, 20 (2013)
3. I. Pâris et al., [SDSS], Astron. Astrophys. **613**, A51 (2018)
4. D.M. Scolnic et al., [Pan-STARRS1], Astrophys. J. **859**(2), 101 (2018)
5. K.S. Dawson et al., [BOSS], Astron. J. **145**, 10 (2013)
6. J.E. Bautista, M. Vargas-Magaña, K.S. Dawson, W.J. Percival, J. Brinkmann, J. Brownstein, B. Camacho, J. Comparat, H. Gil-Marín, E.M. Mueller et al., Astrophys. J. **863**, 110 (2018)
7. S.H. Suyu, V. Bonvin, F. Courbin, C.D. Fassnacht, C.E. Rusu, D. Sluse, T. Treu, K.C. Wong, M.W. Auger, X. Ding et al., Mon. Not. R. Astron. Soc. **468**(3), 2590–2604 (2017)
8. E.J. Baxter et al., [DES], Phys. Rev. D **99**(2), 023508 (2019)
9. P.A.R. Ade et al., [Planck], Astron. Astrophys. **594**, A27 (2016)
10. B.P. Abbott et al., [LIGO Scientific and Virgo], Phys. Rev. Lett. **116**(13), 131103 (2016)
11. B.P. Abbott et al., [LIGO Scientific and Virgo], Phys. Rev. Lett. **116**(6), 061102 (2016)
12. J.A. Vázquez, L.E. Padilla, T. Matos, Rev. Mex. Fis. E **17**(1), 73–91 (2020)
13. B. Si Lakhal, A. Guezmir, J. Phys. Conf. Ser. **1269**(1), 012017 (2019)
14. V.F. Mukhanov, G.V. Chibisov, JETP Lett. **33**, 532–535 (1981)
15. W.H. Press, Phys. Scr. **21**, 702 (1980)
16. A. Bose, S. Chakraborty, Phys. Dark Univ. **35**, 100938 (2022)
17. V. Kamali, M. Motaharfar, R.O. Ramos, Universe **9**, 124 (2023)
18. M. Blagojevic, F.W. Hehl, arXiv:1210.3775 [gr-qc]
19. F.W. Hehl, P. Von Der Heyde, G.D. Kerlick, J.M. Nester, Rev. Mod. Phys. **48**, 393–416 (1976)
20. I.L. Shapiro, Phys. Rep. **357**, 113 (2002)
21. N.J. Popławski, Phys. Lett. B **694**, 181–185 (2010) (**Erratum: Phys. Lett. B 701, 672–672 (2011)**)
22. D. Kranas, C.G. Tsagas, J.D. Barrow, D. Iosifidis, Eur. Phys. J. C **79**(4), 341 (2019)
23. T.M. Guimarães, Rd.C. Lima, S.H. Pereira, Eur. Phys. J. C **81**(4), 271 (2021)
24. M. Tsamparlis, Phys. Rev. D **24**, 1451–1457 (1981)
25. A. Bose, S. Chakraborty, Eur. Phys. J. C **80**(3), 205 (2020)
26. J.D. Barrow, C.G. Tsagas, G. Fanaras, Eur. Phys. J. C **79**(9), 764 (2019)
27. S.H. Pereira, R.C. Lima, J.F. Jesus, R.F.L. Holanda, Eur. Phys. J. C **79**(11), 950 (2019)
28. C.M.J. Marques, C.J.A.P. Martins, Phys. Dark Univ. **27**, 100416 (2020)
29. S. Capozziello, R. Cianci, C. Stornaiolo, S. Vignolo, Phys. Scr. **78**, 065010 (2008)
30. K. Pasmatsiou, C.G. Tsagas, J.D. Barrow, Phys. Rev. D **95**(10), 104007 (2017)
31. M. Bastero-Gil, S. Bhattacharya, K. Dutta, M.R. Gangopadhyay, JCAP **02**, 054 (2018)
32. Y. Zhang, JCAP **03**, 023 (2009)
33. K.V. Berghaus, P.W. Graham, D.E. Kaplan, JCAP **03**, 034 (2020)
34. S. Das, R.O. Ramos, Phys. Rev. D **103**(12), 123520 (2021)
35. Y. Akrami et al., [Planck], Astron. Astrophys. **641**, A10 (2020)
36. H. Sheikhahmadi, A. Mohammadi, A. Aghamohammadi, T. Harko, R. Herrera, C. Corda, A. Abebe, K. Saaidi, Eur. Phys. J. C **79**(12), 1038 (2019)
37. T. Harko, H. Sheikhahmadi, Eur. Phys. J. C **81**(2), 165 (2021)
38. T. Brinckmann, J. Lesgourgues, Phys. Dark Univ. **24**, 100260 (2019)
39. S. Alam et al., [BOSS], Mon. Not. R. Astron. Soc. **470**(3), 2617–2652 (2017)
40. A.J. Ross, L. Samushia, C. Howlett, W.J. Percival, A. Burden, M. Manera, Mon. Not. R. Astron. Soc. **449**(1), 835–847 (2015)
41. A.G. Riess, L. Macri, S. Casertano, H. Lampeitl, H.C. Ferguson, A.V. Filippenko, S.W. Jha, W. Li, R. Chornock, Astrophys. J. **730**, 119 (2011)